

Spatial variation in shallow sediment methane sources and cycling on the Alaskan Beaufort Sea Shelf/Slope



Richard B. Coffin^{a,*}, Joseph P. Smith^b, Rebecca E. Plummer^c, Brandon Yoza^d,
Randolph K. Larsen^e, Lewis C. Millholland^f, Michael T. Montgomery^g

^a Marine Biogeochemistry, Naval Research Laboratory, NRL Code 6114, 4555 Overlook Ave, SW, Washington, DC 20375, USA

^b Department of Oceanography, US Naval Academy, Annapolis, MD, USA

^c Department of Chemistry, University of Maryland, College Park, MD, USA

^d Hawaii Natural Energy Institute, University of Hawaii, Honolulu, HI, USA

^e Department of Chemistry & Biochemistry, St. Mary's College of Maryland, St. Mary's City, MD, USA

^f SAIC c/o Naval Research Laboratory, Washington, DC, USA

^g Marine Biogeochemistry, Naval Research Laboratory, Washington, DC, USA

ARTICLE INFO

Article history:

Received 4 October 2012

Received in revised form

2 May 2013

Accepted 3 May 2013

Available online 18 May 2013

Keywords:

Methane flux

Carbon cycling

Arctic coastal ocean

Arctic shelf

ABSTRACT

The MITAS (Methane in the Arctic Shelf/Slope) expedition was conducted during September, 2009 on-board the U.S. Coast Guard Cutter (USCGC) *Polar Sea* (WAGB-11), on the Alaskan Shelf/Slope of the Beaufort Sea. Expedition goals were to investigate spatial variations in methane source(s), vertical methane flux in shallow sediments (<10 mbsf), and methane contributions to shallow sediment carbon cycling. Three nearshore to offshore transects were conducted across the slope at locations approximately 200 km apart in water column depths from 20 to 2100 m. Shallow sediments were collected by piston cores and vibracores and samples were analyzed for sediment headspace methane (CH₄), pore-water sulfate (SO₄²⁻), chloride (Cl⁻), and dissolved inorganic carbon (DIC) concentrations, and CH₄ and DIC stable carbon isotope ratios (δ¹³C). Downward SO₄²⁻ diffusion rates estimated from sediment pore-water SO₄²⁻ profiles were between -15.4 and -154.8 mmol m⁻² a⁻¹ and imply a large spatial variation in vertical CH₄ flux between transects in the study region. Lowest inferred CH₄ fluxes were estimated along the easternmost transect. Higher inferred CH₄ flux rates were observed in the western transects. Sediment headspace δ¹³C_{CH₄ values ranged from -138 to -48‰, suggesting strong differences in shallow sediment CH₄ cycling within and among sample locations. Measured porewater DIC concentrations ranged from 2.53 mM to 79.39 mM with δ¹³C_{DIC} values ranging from -36.4‰ to 5.1‰. Higher down-core DIC concentrations were observed to occur with lower δ¹³C where an increase in δ¹³C_{CH₄ was measured, indicating locations with active anaerobic oxidation of methane. Shallow core CH₄ production was inferred at the two western most transects (i.e. Thetis Island and Halkett) through observations of low δ¹³C_{CH₄ coupled with elevated DIC concentrations. At the easternmost Hammerhead transect and offshore locations, δ¹³C_{CH₄ and DIC concentrations were not coupled suggesting less rapid methane cycling. Results from the MITAS expedition represent one of the most comprehensive studies of methane source(s) and vertical methane flux in shallow sediments of the U.S. Alaskan Beaufort Shelf to date and show geospatially variable sediment methane flux that is highly influenced by the local geophysical environment.}}}}

© 2013 Published by Elsevier Ltd.

1. Introduction

Global estimates of total methane (CH₄) content in coastal marine sediment hydrates vary greatly, with the most commonly-cited

values ranging from 2600 to 210,000 Gt-C equivalent (Kvenvolden, 1999, 2002; Milkov and Sassen, 2003; Boswell and Collett, 2011). Though the Arctic Ocean is only 1% of the total Earth ocean volume, discrete high porosity and permeable lithologies often saturate coastal ocean and permafrost sediment with gas hydrate (Collett, 2009), making the Arctic Ocean a key region for CH₄-hydrate energy exploration and research on the role of CH₄-hydrate in global climate change. Past studies on climate change in the Arctic tend to

* Corresponding author. Tel.: +1 202 767 0065; fax: +1 202 404 8119.

E-mail address: richard.coffin@nrl.navy.mil (R.B. Coffin).

assume that the land interface is the dominant CH₄ source to the atmosphere (Gorham, 1991; Oechel and Vourlitis, 1994; Frey and Smith, 2005). However, with many coastal regions showing active sediment CH₄ fluxes (i.e. Shakhova et al., 2010), there is a need to evaluate the contribution of Arctic Ocean sediment CH₄ flux to water column carbon cycling and the atmosphere (Isaksen et al., 2011).

Gas hydrate in coastal Arctic oceans occurs primarily in two different geologic settings. Nearshore, gas hydrate is expected to occur at high saturation in sand-rich units as an offshore extension of well-documented terrestrial permafrost-gas hydrate occurrences such as those along the North Slope of Alaska, northern Canada, and Siberia (Collett, 2009). A recent review of multichannel seismic data found the minimum expansion of subsea permafrost does not extend past the 20 m isobath along the Alaskan Shelf, Beaufort Sea (Brothers et al., 2012). Further offshore, gas hydrate exists in deep water settings as a result of higher pressures. In the Arctic Ocean, these conditions extend to somewhat shallower water (~300 m) due to typically lower bottom-water temperature. These deep water hydrates settings impinge on the slope but do not extend onto the shelf. Further evaluation of Arctic Ocean deep sediment hydrate distribution and stability is needed to determine potential changes in ecosystem carbon cycling, relative to tundra extensions of permafrost hydrates to coastal regions, during future warming (Biastoch et al., 2011).

This study presents a spatial overview of variation in the upward vertical CH₄ flux, estimated with a review of sediment CH₄, pore-water sulfate (SO₄²⁻), and dissolved inorganic carbon (DIC) concentrations and stable carbon isotope analyses (Borowski et al., 1996) across the Alaskan Beaufort Sea, during the September 2009 MITAS (Methane in the Arctic Shelf/Slope) expedition, conducted aboard USCGC *Polar Sea* (WAGB-11). At stable gas hydrate pressure-temperature conditions the shallow sediment CH₄ suggests locations with sediment hydrate loadings (Borowski et al.,

1996, 1999; Coffin et al., 2006, 2008). Core samples were collected that cross between boundaries from permafrost to deep ocean hydrates (Brothers et al., 2012), and these results show geospatially variable sediment methane flux that is highly influenced by the unique, local geophysical environment. The MITAS expedition was one of the most ambitious and comprehensive research expeditions to date to investigate spatial variation in methane source(s), vertical methane flux in shallow sediments (<10 mbsf), and methane contributions to shallow sediment carbon cycling on the U.S. Alaskan Beaufort Shelf/Slope.

2. Methods

2.1. Study area overview

The Beaufort Sea (Fig. 1) extends to the northeast from Point Barrow, Alaska to Prince Patrick Island, southward toward Banks Island and westward to the Chukchi Sea, covering 476,000 km² with an average depth of 1004 m. The average shelf width on the U.S. Alaskan region of the Beaufort Sea is 75 km with a coastal westward current that is bordered by the Beaufort Gyre. This base-geology of the shelf plain is mantled with up to hundreds of meters of unconsolidated clastic materials sourced from the Gubik Formation (Engels et al., 2008). Surficial sediment deposits are highly heterogeneous (Naidu and Mowatt, 1983). Over consolidated silty-clay sediment is abundant through this region (Reimnitz and Barnes, 1974). Sediment characteristic in this region is controlled by dispersal and re-suspension of river-borne sediments, ice-scouring, and coastal erosion and retreat (reviewed in Carmack and MacDonald, 2002; Naidu and Mowatt, 1983). Ice-scouring during the last glaciation was dominated by the northwestern progression of the Laurentide ice sheet (Engels et al., 2008). Modern Holocene sediment supply on the shelf is primarily from the two major river systems, the Mackenzie and Colville Rivers. In the

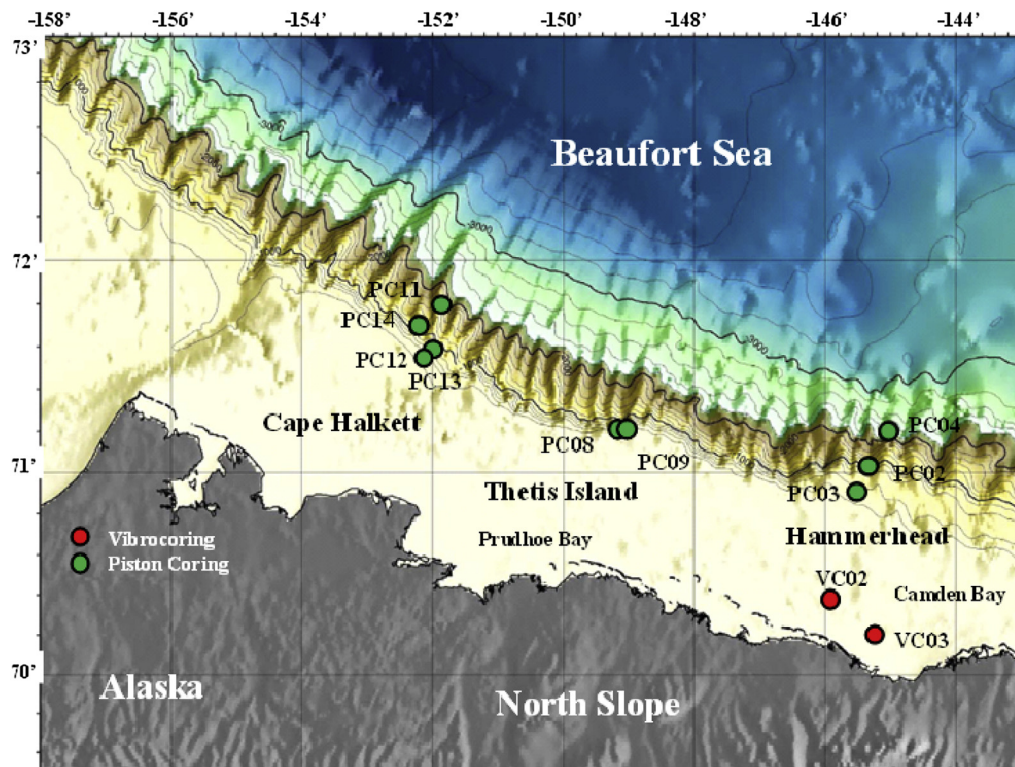


Figure 1. Location of piston core and vibracore sites through Coastal Beaufort Sea in the Arctic Ocean.

Canadian Beaufort Sea, sediment deposited through the Holocene included terrestrial organic carbon from the Mackenzie River at a rate of up to approximately 130–160 tones a^{-1} (Carmack and MacDonald, 2002). In general, the shallow shelf sediments are predominantly clay/silt with some sand and gravel from ice rafting in a few locations, overlain by a thin veneer of finer grained Holocene marine sediment. West of the Mackenzie River system, Beaufort Shelf sediment is deposited from numerous, smaller Arctic river systems including the Colville River (Dunton et al., 2006). Previously-published seismic data showing bottom simulating reflectors (BSRs) along the Shelf/Slope westward of the Colville River infer gas hydrate deposits lying 300 to 700 m below the sea floor with overlying water column ranging from 400 to 2900 m (Andreassen et al., 1997). A thorough review of seismic data in this region indicates that tundra permafrost does not extend beyond a water column depth greater than 20 m (Brothers et al., 2012).

Selection of sampling transects and coring locations was based on a review of Bureau of Ocean Energy Management and U.S. Geological Survey seismic data and onboard analysis of real-time 3.5 kHz acoustic data. Three coring transects were chosen to cover a wide geographic area of the Alaskan Beaufort Shelf/Slope. The transects were named for their general location and proximity to man-made or natural geographic references as: 1) the Hammerhead Line; 2) the Thetis Island Line, and; 3) the Cape Halkett Line (Fig. 1, Table 1). At sites along each transect, seismic profiles identified shallow sediment gas pockets in the permafrost and the top of gas hydrate stability (TGHS) zone in nearshore locations potentially indicative of areas with elevated vertical methane flux. At offshore sites, data review revealed Bottom Simulating Reflectors (BSRs) and regions with seismic blanking as potential indicators of active vertical fluid motion and/or diffusive gas flux.

At the Hammerhead site, nearshore vibracore points (VC02 and VC03) were selected based on seismic and borehole data from previous exploration drilling. Moving offshore on the Hammerhead Line, piston coring locations (PC02, PC03 and PC04) were selected at water column depths of 490–2077 m. To the west of the Hammerhead Line, the Thetis Island transect line was delineated by piston coring sites PC08 and PC09 moving offshore in water depths of 144.5 m and 306 m, respectively. Finally, the Western most Cape Halkett transect line included four piston coring locations (PC11, PC12, PC13, PC14) at water column depths ranging from 280 to 1957 m (Table 1, Fig. 1).

2.2. Core processing and sample collection

Sediment cores were collected using a piston corer (PC) and/or vibracore (VC) fitted with 3 m long – 2.75" I.D. and 9 m long – 3.65"

I.D. (respectively) clear acetate-butyrate core liners. Actual core lengths collected ranged from 105 to 675 cm, with an average of ~400 cm (Fig. 2). Free and sedimentary gases were sampled from holes drilled in whole round core sections. Sediment plugs were collected at distinct sampling intervals in a 3 mL polyethylene syringe with the end cut off, and transferred to pre-weighed 20 mL serum vials from each section to measure the headspace CH_4 concentrations (Hoehler et al., 2000). In select cores, where gas pockets or cracks were clearly visible, free (CH_4) gas was sampled using a gas tight syringe.

After gas collection, cores were then cut into 1 m lengths and split on a horizontal core splitter. Sediment sections were sampled from each core at intervals ranging from 5 to 60 cm. Sediment porewater was sampled from one of the two split halves using Rhizon syringe extractions (Dickens et al., 2007; Seeberg-Elverfeldt et al., 2005). Approximately 5 g of wet sediment were sub-sampled from the other half of each split core section for the determination of porosity and other physical properties. Porewater and sediment sampling intervals were based on appearance of gas pockets or cracks in the sediment, presence of dark (black) sediment, and hydrogen sulfide odor (indicating sulfide production).

After extraction, porewater was dispensed into 1–10 mL vials for subsequent analysis. Headspace CH_4 and porewater sulfate (SO_4^{2-}), chloride (Cl^-), and dissolved inorganic carbon (DIC) concentrations were determined shipboard to estimate the vertical CH_4 flux and to assist in the selection of core sites. Sediment sub-samples and additional porewater sub-samples were stored and shipped at -20°C for sediment porosity determination and $\delta^{13}\text{C}$ analysis.

2.3. Sample analysis

Sediment CH_4 concentrations were measured according to a headspace technique (Hoehler et al., 2000) and quantified using certified gas standards (Scott Gas). Samples were chemically separated using a Shimadzu GC-14A gas chromatograph (GC) equipped with a flame ionization detector and Hayesep-Q 80/100 column. Field data were corrected using sediment porosity data measured post-cruise. The limit of detection (LOD) for CH_4 concentrations was 0.009 mM. Methane concentrations are presented in millimolar units (mM).

Porewater SO_4^{2-} and Cl^- concentrations were measured with a Dionex DX-120 ion chromatograph equipped with an AS-9HC column, Anion Self-Regenerating Suppressor (ASRS Ultra II), and an AS-40 autosampler using a method modified from Paull et al. (2005). Samples were diluted 1:50 (vol/vol) prior to analysis and measured using standard solutions referenced against 1:50 diluted International Association for the Physical Sciences of the Oceans standard seawater (28.9 mM SO_4^{2-} , 559 mM Cl^-). Analytical precision was $\pm 5\%$ of the reference standard. The porewater SO_4^{2-} gradient and depth of depleted SO_4^{2-} concentrations (LOD ~ 0.6 mM) were used to estimate the downward SO_4^{2-} diffusion rate and the approximate depth of the Sulfate Methane Transition (SMT). Chloride concentrations were used to assess potential porewater advection, hydrate dissociation, and of the contribution of tundra-sourced hydrates to coastal sediment porewaters.

Porewater DIC concentrations were determined with a coulometer (UIC) and quantified against certified reference seawater (Scripps Institution of Oceanography, University of California, San Diego, CA). Conversion of DIC to CO_2 and separation from interfering sulfides was conducted according to Boehme et al. (1996). Briefly, a phosphoric acid (10%) solution saturated with CuSO_4 was added to samples to convert DIC to CO_2 and precipitate total dissolved sulfide. CO_2 was transferred to the coulometer with purified nitrogen gas. Concentrations and LOD for DIC was calculated to be 0.23 mM.

Table 1

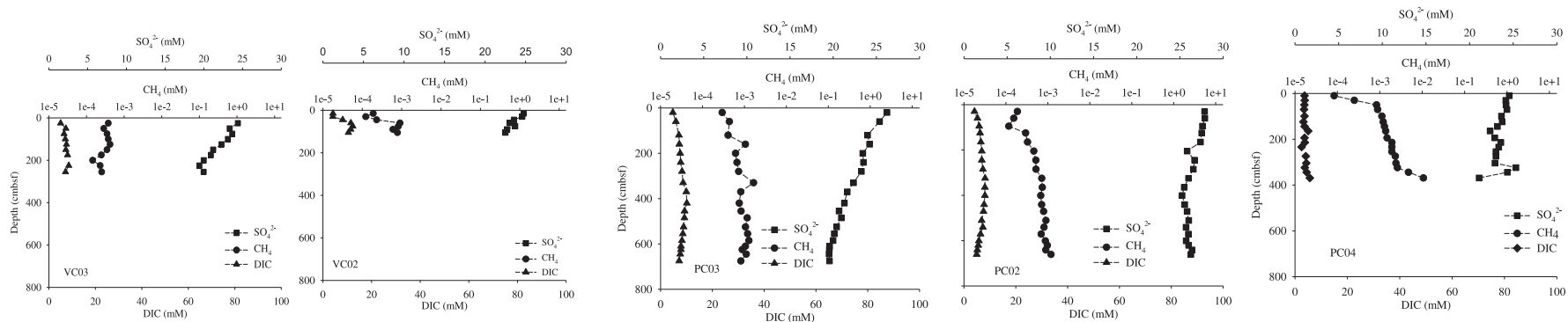
Core date, location, water column depth and chloride. Abbreviations with the cores represent the three different study regions across the Alaskan Shelf in the Beaufort Sea; Cape Halkett (CH), Thetis Island (TI) and Hammerhead (H).

Core	Date	Latitude	Longitude	Depth (m)	Chloride (mM)
VC02, H	19-Sep-09	70°21.64480'N	146°00.46350'W	20	484 ± 11
VC03, H	19-Sep-09	70°15.34210'N	146°04.69180'W	22	482 ± 7
PC02, H	20-Sep-09	71°00.22810'N	145°27.03660'W	566	543.6 ± 7
PC03, H	20-Sep-09	70°58.47840'N	145°29.21420'W	490	505 ± 5
PC04, H	21-Sep-09	71°11.98460'N	145°14.95110'W	2077	470 ± 17
PC08, TI	23-Sep-09	71°12.44330'N	149°13.46600'W	144.5	490 ± 8
PC09, TI	23-Sep-09	71°13.14430'N	149°13.23340'W	306	521 ± 5
PC11, CH	25-Sep-09	71°46.68280'N	151°52.70670'W	1458	519 ± 5
PC12, CH	25-Sep-09	71°32.97120'N	152°03.68110'W	342	517 ± 7
PC13, CH	25-Sep-09	71°31.86300'N	152°04.75420'W	280	499 ± 6
PC14, CH	25-Sep-09	71°37.64200'N	151°59.29430'W	1005	509 ± 4

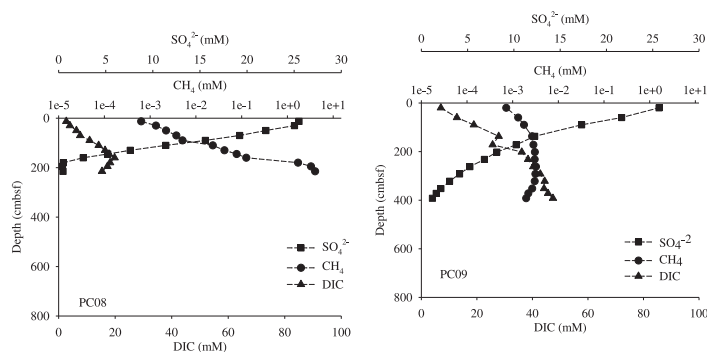
Nearshore



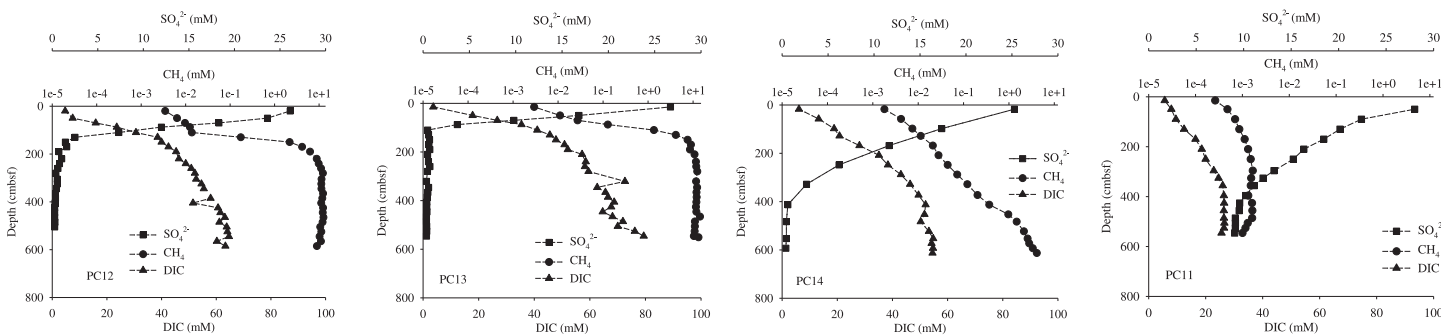
Offshore



Hammerhead



Thetis Island



Cape Halkett

Figure 2. Core porewater profiles for CH_4 , SO_4^{2-} and DIC at the Cape Halkett, Thetis Island, Hammerhead nearshore and Hammerhead offshore location.

For $\delta^{13}\text{C}_{\text{DIC}}$ analysis, an excess of 85% phosphoric acid was added to a 2 mL serum vial containing 1.5 mL of porewater to convert DIC to CO_2 . Vials were shaken to purge the CO_2 into the headspace. Samples were injected into the split/splitless injector of a Thermo Trace GC, and CO_2 was separated with a Varian Porapak-Q column (25 m, 0.32 mm id). $\delta^{13}\text{C}_{\text{DIC}}$ values were measured with a Delta Plus XP I isotopic Ratio Mass Spectrometer (IRMS) (Thermo). Measured $\delta^{13}\text{C}$ values were standardized using tank CO_2 referenced to the NIST RM 8560 natural gas standard.

Headspace and free-gas $\delta^{13}\text{C}_{\text{CH}_4}$ values were determined using a Thermo Trace GC interfaced via a GC-C III combustion unit to a Delta Plus XP IRMS (Plummer et al., 2005; Coffin et al., 2008). Samples were injected into a helium stream and cryogenically concentrated on a 3 cm segment of Porapak-Q column (0.32 mm id) immersed in liquid nitrogen (Plummer et al., 2005). All $\delta^{13}\text{C}_{\text{CH}_4}$ values were measured against CO_2 reference gas, which was normalized to the Vienna Pee Dee Belemnite (VPDB) scale through analysis of a certified natural gas standard (NIST RM 8560).

Sediment porosity (ϕ) was measured gravimetrically (Hoehler et al., 2000; Coffin et al., 2008). Sediment water content was determined assuming constant porewater and bottom water density and then ϕ was calculated using a constant solid matter density (ρ_{sm}) of 2.50 g/cm³.

3. Results

Sediment headspace CH_4 concentration in cores ranged from LOD to 14.24 mM (Fig. 2). Lowest concentrations, up to 0.01 mM, were measured in nearshore and offshore cores from the Hammerhead Line (VC03, VC04, PC02, PC03, and PC04, Fig. 2). In cores collected along the Thetis Island Line (PC08, PC09), headspace CH_4 concentrations ranged from LOD to 4.02 mM with highest at PC08 (Fig. 2). Headspace CH_4 concentrations in cores along the Cape Halkett Line ranged from LOD to 14.24 mM, with higher concentrations in deeper core sections. Cores PC12 and PC13, located at the more shallow water column depths, had the highest headspace CH_4 concentrations measured at the Cape Halkett site (and highest of any cores collected during the MITAS expedition) while PC11 and PC14, located in deeper waters, were lowest (Fig. 2, Table 1). The general trend in headspace CH_4 vertical profiles in all cores showed lowest concentrations in shallow sediments with an increase at mid-core depths.

Porewater SO_4^{2-} concentrations in cores ranged from LOD to 26.7 mM (Fig. 2). Concentrations for Hammerhead nearshore cores (VC02, VC03) ranged from 24.7 mM at surface down to 19.4 mM, in VC03. Sediment porewater concentrations in the offshore cores from the Hammerhead Line were near typical seawater values of 26.5 mM in sections close to the sediment–water interface decreasing slowly with depth to a down-core minimum of 19.6 mM at 675 cmbsf (PC03). At Thetis Island, porewater SO_4^{2-} concentrations decreased much more rapidly with depth, reaching LOD mid-core at 180 cmbsf in PC08 and at 392 cmbsf for PC09. Shallowest SO_4^{2-} profiles were in cores from the Cape Halkett Line with minimum concentrations of 9.1 mM at 546 cmbsf in the furthest offshore core, PC11. In cores from the Cape Halkett Line closer to shore, up the slope, concentrations reached below LOD at 405, 110 and 220 cmbsf for PC12, PC13 and PC14, respectively. Trends in the SO_4^{2-} profile varied among the different regions (Fig. 2). At Hammerhead profiles showed little change with depth and did not reach LOD. Westward at Thetis Island, a rapid shift in the profiles was observed with steeper slopes reaching SO_4^{2-} LOD. Further westward at Cape Halkett SO_4^{2-} minimums were shallower nearshore. However, offshore SO_4^{2-} profiles were non-linear and did not reach LOD.

Average porewater Cl^- concentrations measured in the sediment cores collected ranged between 470 ± 17 to 543.6 ± 7 mM (Table 1). The highest porewater Cl^- values were in offshore cores (PC11, PC14) from the Cape Halkett Line while lowest values were in nearshore cores (VC-02, 03; PC-04) from the Hammerhead Line (Table 1, Fig. 1). In general, sediment porewater Cl^- concentrations increased nearshore to offshore with PC04 on the Hammerhead Line being a notable exception (Table 1).

Measured porewater DIC values in the sediment cores ranged from 2.53 to 79.39 mM (Fig. 2). Low porewater DIC concentrations were measured in the nearshore cores from the Hammerhead Line (VC02 and VC03; range 4.06–12.29 mM) with minimum values near the surface that increased slightly with depth. Measured porewater DIC concentrations at the Hammerhead Line offshore cores (PC03 and PC04) were typically lower (2.53–10.16 mM) and showed little variation vertically. Moving westward to Thetis Island Line cores, porewater DIC concentration in cores PC08 and PC09 rapidly increased with depth to 19.8 mM at 160 cmbsf in PC08 and 47.4 mM at 392 cmbsf in PC09. Porewater DIC concentration generally varied with sediment headspace CH_4 profiles and inversely with porewater SO_4^{2-} profiles (Fig. 2). DIC concentrations continued to increase moving further west to the Cape Halkett cores (PC12 and PC13), increasing rapidly at the bottom of both cores up to as high as 79.39 mM.

Average sediment ϕ ranged from 0.422 ± 0.037 to 0.718 ± 0.034 (Table 2) with the highest values in cores collected along the westward Cape Halkett Line. At this location, values increased from 0.659 ± 0.023 in PC12 closer to the shelf break to 0.718 ± 0.032 in PC-11 from the slope. Lowest sediment ϕ values were at nearshore Hammerhead core sites (VC-02) with a minimum value of 0.422 ± 0.037 at VC02 (Table 2). Other notable low average sediment ϕ values were in the PC08 core from the Thetis Island Line (0.509 ± 0.084) and the PC04 (0.475 ± 0.029) core from the Hammerhead Line.

Sulfate diffusion rates were estimated by plotting a regression line, relative to depth, using porewater SO_4^{2-} concentrations that ranged from -1.9 to -154.8 mmol $\text{m}^{-2} \text{a}^{-1}$ (Table 2). Lowest diffusion rates were at the offshore Hammerhead site with a range of -1.9 to -6.1 mmol $\text{m}^{-2} \text{a}^{-1}$. Moving inshore at the Hammerhead site there was a moderate increase to -15.4 mmol $\text{m}^{-2} \text{a}^{-1}$. Moving westward, estimated SO_4^{2-} diffusion rate increased, with maximum values of -100.1 mmol $\text{m}^{-2} \text{a}^{-1}$ and -154.8 mmol $\text{m}^{-2} \text{a}^{-1}$ at the Thetis Island and Cape Halkett Lines, respectively. At both of these westward locations, the highest SO_4^{2-} flux rates were at shallow core points. Methane profiles were compared with sulfate profiles to estimate SMT depth at Thetis Island and Cape Halkett (Table 2). A minimum SMT depth (106 cmbsf) was at Cape Halkett PC13 while deepest SMTs were further offshore (629 cmbsf, PC11).

Table 2

Estimates of the sulfate-methane-transition (SMT), downward sulfate diffusion, sediment porosity for core locations in the Beaufort Sea. Abbreviations with the cores represent the three different study regions across the Alaskan Shelf in the Beaufort Sea; Cape Halkett (CH), Thetis Island (TI) and Hammerhead (H).

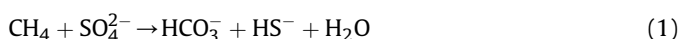
Core	SMT (cmbsf)	SO_4^{2-} (mmol $\text{m}^{-2} \text{a}^{-1}$)	Average porosity
VC02, H	–	–15.4	0.482 ± 0.057
VC03, H	–	–15.2	0.422 ± 0.037
PC02, H	–	–1.9	0.635 ± 0.089
PC03, H	–	–6.1	0.642 ± 0.076
PC04, H	–	–2.1	0.509 ± 0.084
PC08, TI	179	–100.1	0.475 ± 0.029
PC09, TI	351	–37.7	0.664 ± 0.017
PC11, CH	629	–27.4	0.718 ± 0.032
PC12, CH	147	–124.7	0.672 ± 0.024
PC13, CH	106	–154.8	0.659 ± 0.023
PC14, CH	373	–44.2	0.709 ± 0.034

$\delta^{13}\text{C}_{\text{CH}_4}$ of gas collected from pockets in the PC12 core from the Cape Halkett Line was $-84.4 \pm 0.5\text{‰}$ ($n = 12$). $\delta^{13}\text{C}_{\text{CH}_4}$ for sediment headspace CH_4 in all cores ranged from -137.2‰ to -48.2‰ , when detectable (Fig. 3). A general trend through all cores was that $\delta^{13}\text{C}_{\text{CH}_4}$ were enriched in shallow sediment and depleted with depth. An exception to this trend was in the PC12 and PC13 cores from the Cape Halkett Line, where $\delta^{13}\text{C}_{\text{CH}_4}$ was depleted to -100‰ at 150 and 110 cmbsf, respectively, followed by ^{13}C enrichment to -82.7‰ down core. Lowest $\delta^{13}\text{C}_{\text{CH}_4}$ in all cores was at PC04, -137.2‰ at 190 cmbsf, offshore at the Hammerhead Line (Fig. 3).

$\delta^{13}\text{C}_{\text{DIC}}$ in porewater varied from 5.1‰ to -36.3‰ along vertical profiles among all locations (Fig. 3). In all cores, porewater $\delta^{13}\text{C}_{\text{DIC}}$ near the sediment water interface were near typical seawater values (-10 to 0‰). Cores collected along the Hammerhead Line (VC02, VC03, PC02, PC03, PC04) showed profiles that were gradually ^{13}C -depleted from the surface to deep porewater with little change in $\delta^{13}\text{C}_{\text{DIC}}$ values with depth (Fig. 3). Porewater DIC collected along the Thetis Island and Cape Halkett Lines that had significant CH_4 concentrations (PC08, PC12, PC13) was much more ^{13}C -depleted ($\sim -40\text{‰}$ to -20‰) towards and through the apparent SMT. The PC08 core from the Thetis Island Line showed shallow, rapid ^{13}C -depletion to $\sim -40.0\text{‰}$ at the SMT at ~ 150 cmbsf, then rapid ^{13}C -enrichment to $\sim -22.0\text{‰}$ from the SMT to core base (~ 200 cm). Likewise, Cape Halkett cores PC12 and PC13 showed rapid ^{13}C -depletion down to $\sim -21.0\text{‰}$ at the SMT between 80 and 130 cmbsf that shifted to enriched $\delta^{13}\text{C}_{\text{DIC}}$ values of $+5.1\text{‰}$.

4. Data evaluation

Porewater SO_4^{2-} profiles in shallow sediments over deep hydrates are dependent upon the upward vertical CH_4 flux and sediment properties which control the deposition and burial rate of terrestrial and planktonic organic matter, bioturbation and bio-irrigation, and the downward diffusion of seawater SO_4^{2-} from the water column. With strong spatial variation in ice-scouring of surface sediments through this study region we focus on the vertical CH_4 flux observed by the linear slopes of vertical SO_4^{2-} profiles (Borowski et al., 1999; Coffin et al., 2008). Porewater SO_4^{2-} concentrations generally decrease through the shallow sediment as SO_4^{2-} is consumed as the terminal electron acceptor during decomposition of organic matter via organoclastic sulfate reduction (SR) (Berner, 1964, 1978) or through anaerobic oxidation of methane (AOM) (Borowski et al., 1996, 1999). Organoclastic SR is dominant in many marine locations though SR may be coupled with AOM in the presence of CH_4 (Borowski et al., 1999; Aharon and Fu, 2000; Valentine and Reeburgh, 2000; Orphan et al., 2001; Valentine, 2002; Coffin et al., 2008). In sediments with vertical CH_4 flux, AOM may be the dominant pathway for SR (Borowski et al., 1996; Boetius et al., 2000; Pancost et al., 2000; Torres et al., 2003; Zhang et al., 2003; Treude et al., 2005; Coffin et al., 2008). In these locations, AOM is conducted by way of a metabolic partnership between methanogen-like archaea that oxidize CH_4 and SO_4^{2-} reducing bacteria (Orphan et al., 2001; Valentine, 2002) and can be described by the following net reaction:



The sedimentary horizon where CH_4 and SO_4^{2-} co-occur and are consumed during AOM is termed the sulfate methane transition (SMT) (Borowski et al., 1999; Valentine, 2002). The depth of the SMT and rates of AOM are controlled by the rate of vertical upward CH_4 and downward SO_4^{2-} diffusion (Borowski et al., 1996, 1999). Assuming a steady-state inverse linear relationship between CH_4

and SO_4^{2-} (Borowski et al., 1996), in which organoclastic SR is constant and the vertical CH_4 gradient vary as a function of the AOM rate, one can use SMT depth and the slope of the downward porewater SO_4^{2-} gradient to estimate SO_4^{2-} diffusion rate from water column into sediment and thus infer upward CH_4 (diffusive) flux. Physical and biological processes, such as slope instability, fluid advection, bioturbation, pulsed inputs of organic matter, and SR not coupled to AOM can result in a non-steady state relationship between SO_4^{2-} and CH_4 profiles that limits using SO_4^{2-} porewater profiles to predict vertical CH_4 flux (Hensen et al., 2003; Joye et al., 2004; Coffin et al., 2006, 2008). The sulfate-methane-transition depth (SMT) was determined as the depth in the sediments where minimum CH_4 and SO_4^{2-} concentrations converge plus half the depth to the next core section (Coffin et al., 2008).

Sulfate diffusion rates were calculated from the linear fit to the SO_4^{2-} concentration gradient according to Fick's first law (Berner, 1964, 1978):

$$J = -\phi \cdot D_s \cdot \frac{dc}{dx} \quad (2)$$

where J represents the SO_4^{2-} flux ($\text{mmol m}^{-2} \text{a}^{-1}$), ϕ is the sediment porosity, D_s is the sediment diffusion coefficient, c is the range in SO_4^{2-} concentration and x is the range in depth for the linear section of the SO_4^{2-} porewater profile. D_s is the diffusion coefficient for SO_4^{2-} :

$$D_s = \frac{D_0}{1 + n(1 - \phi)} \quad (3)$$

where D_0 is assumed to be $8.7 \times 10^{-5} \text{ cm}^2 \text{ s}^{-1}$ (Iversen and Jørgensen, 1993), $n = 3$ was assumed for the clay silt sediments in this region, and ϕ is the sediment porosity determined from core sub-samples. Downward SO_4^{2-} diffusion into the sediment is expressed as negative and upward CH_4 flux is expressed as positive (out of the sediment). Methane flux (diffusive) out of the sediment was inferred from the SO_4^{2-} diffusion rate by assuming a 1:1 ratio of SR to CH_4 oxidation that is typically present during AOM (Equation (1); Borowski et al., 1996; Burdige and Komada, 2011). In sediment cores with non-linear porewater SO_4^{2-} profiles near the sediment surface, deeper, linear portions of the SO_4^{2-} profile below the apparent mixing depth were selected for calculation of SO_4^{2-} diffusion rate (Berner, 1978; Coffin et al., 2008). In sediment cores with clearly non-linear SO_4^{2-} profiles, it was assumed that non-linear and/or non-steady state conditions were present so the SO_4^{2-} diffusion rate, and hence the CH_4 flux, could not be estimated.

5. Discussion

SMT depths and SO_4^{2-} diffusion rates were estimated for cores collected along the Hammerhead, Thetis Island, and Cape Halkett Line (Table 2, Fig. 1). The scale and shape of measured headspace CH_4 and porewater SO_4^{2-} and DIC profiles varied from core-to-core and between different core locations, suggesting a large degree of spatial variability in methane fluxes on the Alaskan Beaufort Shelf (Fig. 2). SMT depth in the sediment can be estimated where headspace CH_4 concentrations approach the LOD in conjunction with a rapid depletion of porewater SO_4^{2-} , assuming steady-state conditions and SO_4^{2-} consumption dominated by AOM (Table 2, Borowski et al., 1996, 1999). Where the lowest sediment headspace CH_4 concentrations were measured through core profiles, there was a shallower slope in the SO_4^{2-} profile and hence a deeper estimated SMT and a lower downward diffusion rate of seawater-derived SO_4^{2-} (Hammerhead Line: VC02, VC03, PC02, PC03, PC04). In contrast, shallow SO_4^{2-} minima were in cores from the Thetis

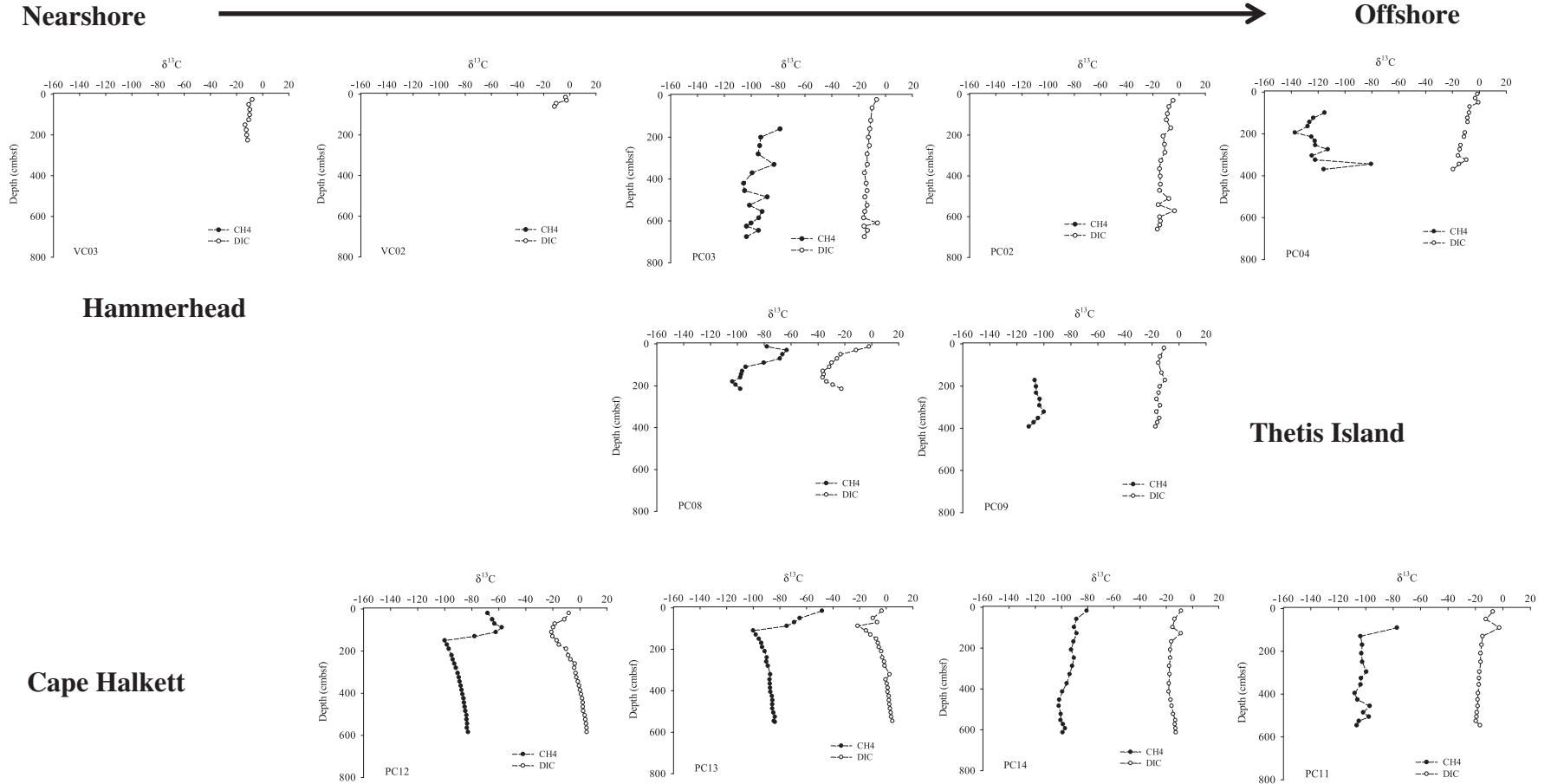


Figure 3. Core porewater $\delta^{13}\text{C}$ profiles for CH₄ and DIC at the Cape Halkett, Thetis Island, Hammerhead nearshore and Hammerhead offshore location.

Island Line (PC08) and the Cape Halkett Line (PC12, PC13) which also had higher headspace CH₄ concentrations. Linear headspace CH₄ and SO₄²⁻ profiles were inversely related in these cores, with especially strong inverted patterns at PC12 and PC13 (Fig. 2) suggesting high rates of AOM (Borowski et al., 1996, 1999; Boetius et al., 2000; Coffin et al., 2008; Knittel and Boetius, 2009).

For cores PC08, PC12, PC13 and PC14, a clear depletion of CH₄ and SO₄²⁻ sourced from deeper sediment and overlying seawater, respectively, was observed and provided a range of SMT estimates from 106 to 373 cmbsf (Table 2). In cores PC09 and PC11, SO₄²⁻ and CH₄ profiles covaried which is indicative of AOM (353 and 629 cmbsf, respectively). Variations in SO₄²⁻ profiles in cores from PC03, PC04, VC02 and VC03 result from variable rates of organoclastic SR and resultant downward SO₄²⁻ diffusion.

Analyses of the spatial variations in porewater SO₄²⁻ profiles provide a general summary among coring sites for AOM and organoclastic SR relative to the downward diffusion of SO₄²⁻ through shallow sediment (Table 2). The lowest SO₄²⁻ diffusion rates were estimated for offshore and nearshore Hammerhead core sites with a minimum of $-2.03 \text{ mmol SO}_4^{2-} \text{ m}^{-2} \text{ a}^{-1}$. More rapid SO₄²⁻ diffusion rates were estimated westward at the Thetis Island Line (PC08, $-100 \text{ mmol m}^{-2} \text{ a}^{-1}$). Further westward, on the Cape Halkett Line, the highest SO₄²⁻ diffusion rates ranged from -17.7 to $-155 \text{ mmol m}^{-2} \text{ a}^{-1}$; with the highest rates at coring sites PC12 and PC13.

Where SO₄²⁻, CH₄ and DIC profiles suggest AOM, estimates of CH₄ flux based on porewater SO₄²⁻ profiles (Table 2) are in the range of recent studies of other coastal regions (Table 3). Active vertical CH₄ diffusion ranged from 6.3 to 362 mmol m⁻² a⁻¹ off the mid Chilean Margin, At water Valley in the Gulf of Mexico, and coast of Uruguay (Hensen et al., 2003; Treude et al., 2005; Coffin et al., 2006, 2008). Rates at deeper coring sites in this study were similar to that in nearby Bering Sea shelf slope of 25.3 mmol m⁻² a⁻¹ (Wehrmann et al., 2011). Substantially lower diffusion rates have been measured in other coastal regions; e.g. 7.2–7.9 mmol m⁻² a⁻¹ on Blake Ridge (Dickens, 2001). Estimated vertical CH₄ fluxes were highly variable at our three regions across the Beaufort Sea. Eastward in the study region, low fluxes similar to those measured on Blake Ridge were estimated at Hammerhead nearshore tundra and offshore slope core sites. Moving westward to Thetis Island and Cape Halkett core sites, estimated vertical CH₄ flux was more rapid and similar to other coastal regions that have deep sediment hydrate deposits that are driving shallow sediment CH₄ cycling. However, this region is likely to have hydrate formation in shallower sediment due to lower temperatures creating stability in more shallow sediment and sediment accumulation during past ice scouring (Engels et al., 2008).

The data in this study are limited given the large area but, in general, shallower SMTs, higher sulfate diffusion rates, and higher inferred CH₄ flux rates were observed moving nearshore to offshore, shelf to slope, and moving east to west from the Hammerhead to Cape Halkett Line (Table 1, Figs. 1 and 2). The reason for this spatial trend is an area of ongoing research by MITAS collaborators. It is likely related to a variety of factors, such as influence of local organic matter methane sources, regional circulation patterns and specialized sediment transport mechanisms (e.g. ice gouging, rafting), as well as the unique geologic and geophysical environment of the U.S. Alaskan Beaufort Shelf/Slope. Coastal erosion in our study area is a substantial input of sediment carbon (Jorgenson and Brown, 2005). Westward deposition results from ice scouring and subsequent glaciogenic sediment beds forming during Pleistocene glacial periods (Engels et al., 2008) could result in the long term organic matter accumulations and subsequent elevated vertical methane flux. Sediment gouging and subsequent ice-rafting is a major sediment transport mechanism along the Beaufort Shelf Slope and could influence organic matter and sediment transport (Naidu and Mowatt, 1983).

Differences in sediment ϕ , suggest some degree of geologic control on sediment CH₄ flux (Table 2). Sediment ϕ was generally lower nearshore and increased offshore at each transect line, with the offshore PC08 site on the Thetis Island Line as the notable exception. The PC08 core was exceptional in that it was more similar to other nearshore cores and it contained firm to very firm, clayey-silt with rare silt lamina, FeS mottling and bands throughout. Shell fragments and organic material were present in the lower half of the core (K. Rose, NETL, unpublished). Also, the gradual freshening of sediment porewaters in cores moving offshore to nearshore, based on Cl⁻ concentrations, might be an indication of permafrost extension out onto the U.S. Alaskan Beaufort Shelf (Table 1). Porewater salinity is known to influence methane hydrate stability and vertical porewater flux rates (Lu and Matsumoto, 2005).

Porewater DIC concentrations and core profiles were consistent with headspace CH₄ and SO₄²⁻ profiles. In cores with measurable headspace CH₄, porewater DIC increased with depth down through the SMT as HCO₃⁻ was released into porewaters in a 1:1 stoichiometry with the consumption of CH₄ and SO₄²⁻ during AOM (Equation (1)). Higher down-core porewater DIC concentrations can be indicative of elevated AOM rates. Interestingly, DIC concentrations were relatively high (up to 79.4 mM) at Cape Halkett (PC12, PC13, PC14) and are remarkably higher than those reported in regions with high CH₄ diffusion rates; e.g. a maximum of 20–40 mM DIC in other coastal regions (Coffin et al., 2006, 2008; Arvidson et al., 2004; Hamdan et al., 2011). Given these DIC

Table 3

Overview of methane SMT and diffusion rates at different coastal regions around the world. The methane diffusion rates are summarized on the basis of downward sulfate diffusion profiles and the assumption of a 1:1 methane:sulfate stoichiometry during AOM.

Location	Minimum SMT (cmbsf)	Maximum SMT (cmbsf)	Minimum diffusion (mM CH ₄ m ⁻² a ⁻¹)	Maximum diffusion (mM CH ₄ m ⁻² a ⁻¹)	Reference
Beaufort Sea	147	2905	2.1	154.8	This study
Mid Chilean Margin	33	1011	13.3	362.0	Coffin et al., 2006
Atwater Valley, Gulf of Mexico	0	410	20.4	249.1	Coffin et al., 2008
Kara, Chukchi and White Seas	–	–	0.44	47.4	Lein et al., 2011
Hikurangi Margin, New Zealand	183	1287	11.4	86.2	Coffin et al., 2007
Alaminos Canyon, Gulf of Mexico	308	1793	–	–	Coffin et al., 2007
Umitaka Spur, Japan	200	300	58	102	Snyder et al., 2007
Western Argentine Basin	370	22,000	1	162.5	Hensen et al., 2003
Garden Banks and Mississippi Canyon, Gulf of Mexico	~100	~250	–	–	Ruppel et al., 2005
Southern Chilean Margin	–	–	46	100	Treude et al., 2005
Bering Sea Slope	6	–	–	25.3	Wehrmann et al., 2011

concentrations were higher than CH₄ through the profiles, there is likely an alternate (bio-) geochemical cycle or allochthonous source contributing to porewater DIC.

$\delta^{13}\text{C}$ of CH₄ and DIC values can be used to delineate CH₄ sources and cycling between the three transect lines in this study. $\delta^{13}\text{C}_{\text{CH}_4}$ of PC12 gas pockets ($-84.4 \pm 0.5\%$, $n = 12$) and a C1/C2 ratio of 89,000 for PC8, PC11, PC12 and PC13 when ethane was present indicates a biogenic methane source at these sites. Earlier studies in Mackenzie Delta have also reported biogenic methane to be the dominant gas source (Dallimore and Collett, 1995, 1998). Along with strong variations in CH₄ concentrations, significant $\delta^{13}\text{C}_{\text{CH}_4}$ variation (-137.2% to -48.2%) in samples collected in this study highlights differences between CH₄ production and oxidation in the sediments of the U.S. Alaskan Beaufort Shelf/Slope (Whiticar, 1999, Fig. 3). A general trend through all of the shallow core sections in this study was ^{13}C enrichment from isotopic fractionation during AOM (Hinrichs et al., 1999). There were large shifts in $\delta^{13}\text{C}_{\text{CH}_4}$ vertical profiles at PC12 and PC13. These cores had shallow SMTs and a rapid diffusive CH₄ flux rate as inferred by the steep, linear slope of the porewater SO_4^{2-} profile (Table 2). Another unique observation in the $\delta^{13}\text{C}_{\text{CH}_4}$ profiles was high ^{13}C -depletion mid-profile in PC04, located offshore Hammerhead. This ^{13}C -depleted signature was in the range of 200 cmbsf, well above the predicted SMT of 2905 cmbsf, and suggested shallow sediment CH₄ production. Depleted CH₄ $\delta^{13}\text{C}$ occurs during biogenic methane production in slow diffusive porewater gradients (Martens and Berner, 1974; Wehrmann et al., 2011).

$\delta^{13}\text{C}_{\text{DIC}}$ in sediment porewater ranged from -36.4% to 5.1% (Fig. 3) and often co-varied with $\delta^{13}\text{C}_{\text{CH}_4}$, suggesting varying degrees of CH₄ cycling between locations. In the surface core, $\delta^{13}\text{C}_{\text{DIC}}$ ranged from approximately -10% to 0.5% through the profile with a maximum depletion at 10 cmbsf. Where shallow SMT depths were measured (PC08, PC12, PC13), there was a sharp depletion in $\delta^{13}\text{C}_{\text{DIC}}$, down to -10% resulting from AOM. Finally, at Cape Halkett, with shallow SMT there was a shift in $\delta^{13}\text{C}_{\text{DIC}}$, below the SMT, up to 5.1% from isotope fractionation in the DIC pool that was associated with CH₄ production.

Sources and cycling of CH₄ (Fig. 4) and DIC (Fig. 5) through the core transects are summarized using the following equations (Aller and Blair, 2006; Blair et al., 2003):

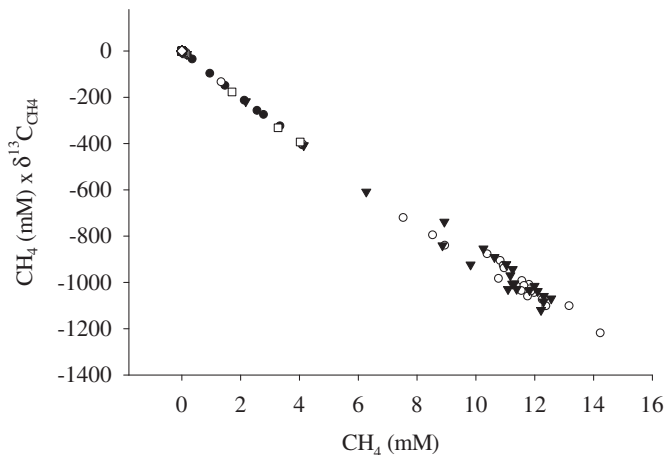
$$C_x = C_a + C_b \quad (4)$$

$$\delta^{13}\text{C}_x C_x = \delta^{13}\text{C}_a C_a + \delta^{13}\text{C}_b C_b \quad (5)$$

$$\delta^{13}\text{C}_x C_x = \delta^{13}\text{C}_a C_a + \delta^{13}\text{C}_b C_b + \delta^{13}\text{C}_\Delta \Delta C \quad (6)$$

$$\frac{d(\delta^{13}\text{C}_x C_x)}{dC} = \delta^{13}\text{C}_\Delta + \frac{d(\delta^{13}\text{C}_\Delta)}{dC} \quad (7)$$

$\delta^{13}\text{C}$ of carbon cycled through C_x (CH₄ and DIC, Equation (4)) was assumed to result from two carbon sources (a and b) concentrations and $\delta^{13}\text{C}$ (Equation (5)). For CH₄ analysis, it was assumed that the source was biogenic and that values are shifted in the sediment profile due to AOM and methanogenic metabolism. This variation can be resolved by comparing CH₄ concentration and $\delta^{13}\text{C}$ by source and degree of fractionation during cycling. For porewater DIC, it was assumed that the source is seawater and microbial respiration vs. autotrophic production is the dominant influence on porewater DIC profiles. With these assumptions for CH₄ and DIC, ΔC represents the quantity of carbon cycled and $\delta^{13}\text{C}_\Delta$ is a net isotopic change (Equation (6)). Assuming $\delta^{13}\text{C}_a C_a$ is constant or zero and ΔC does not equal zero, a linear correlation in this relation provided $\delta^{13}\text{C}_\Delta$ as source carbon cycled through a sediment profile (Equation (7)).



- PC14 - $r^2 = 1.000$, $a = -99.0$
- PC13 - $r^2 = 0.995$, $a = -85.6$
- ▼ PC12 - $r^2 = 0.993$, $a = -86.6$
- △ PC11 - $r^2 = 0.965$, $a = -107.6$
- PC09 - $r^2 = 0.991$, $a = -103.2$
- PC08 - $r^2 = 0.999$, $a = -99.5$
- ◆ PC04 - $r^2 = 0.966$, $a = -109.1$
- ◇ PC03 - $r^2 = 0.914$, $a = -68.0$

Figure 4. $\delta^{13}\text{C}_{\text{CH}_4}$ as a function of CH₄ concentration for source evaluation at each core location.

Based on this data analysis, sediment CH₄ was found to be biogenic across the Alaskan Beaufort Shelf, with a large range in $\delta^{13}\text{C}$ (-107.6% to -68.0% , Fig. 4), suggesting strong spatial variation in CH₄ cycling. Range in $\delta^{13}\text{C}_{\text{CH}_4}$ between locations is controlled by vertical CH₄ flux (Table 2) and AOM. $\delta^{13}\text{C}_{\text{CH}_4}$ enrichment was greatest in shallower depths along the Hammerhead Line, indicative of isotopic enrichment relative to PC13 gas pockets. In all other cores, there was depleted $\delta^{13}\text{C}$ that varied with estimated vertical CH₄ flux. At PC12 and PC13, where the maximum CH₄ diffusion was estimated ($124.7\text{--}154.8 \text{ mM CH}_4 \text{ m}^{-2} \text{ a}^{-1}$), the source $\delta^{13}\text{C}_{\text{CH}_4}$ was -85.6% and -86.6% , similar to $\delta^{13}\text{C}_{\text{CH}_4}$ in PC12 core gas pockets. With a lower CH₄ diffusion rate (PC04, PC09, PC11, PC14), $\delta^{13}\text{C}_{\text{CH}_4}$ was isotopically depleted, indicative of a high shallow sediment CH₄ production. Thetis Island Line core PC08 did not fit this pattern; while there was a relatively shallow SMT that indicated a strong vertical CH₄ flux, other data suggested additional carbon sources and cycles contribute to net carbon cycling.

Relative to $\delta^{13}\text{C}_{\text{CH}_4}$, there appeared to be multiple factors through our study region that influence the porewater DIC pool including AOM, methanogenesis, carbonate dissolution and precipitation, and organoclastic sulfate reduction (Fig. 5). Below the SMT at PC12, PC13 and PC14, $\delta^{13}\text{C}_{\text{DIC}}$ was enriched (up to 39.1%) and $\delta^{13}\text{C}_{\text{CH}_4}$ was depleted (Fig. 4) indicating high rates of methanogenesis within the piston core profile. Below the SMT for PC08 and PC09, DIC was ^{13}C depleted and more characteristic of porewater profiles (Fig. 5). Above the SMT at Cape Halkett, a depth that CH₄ is not present (PC11, PC12, PC13, PC14), there was a strong shift in the DIC signature from seawater toward a value characteristic of a phytoplankton source (Fig. 5, -19.2 to -21.4%). Estimates of pelagic contribution to shallow sediments suggest phytoplankton can contribute up to 56% of carbon in the Beaufort and Chukchi Seas (Belicka et al., 2004). At the Thetis Island Line, $\delta^{13}\text{C}_{\text{DIC}}$ was elevated and more characteristic of seawater $\delta^{13}\text{C}_{\text{DIC}}$ (-11.2% to -1.78% , Fig. 5). With the exception of PC04, there was not a large change in

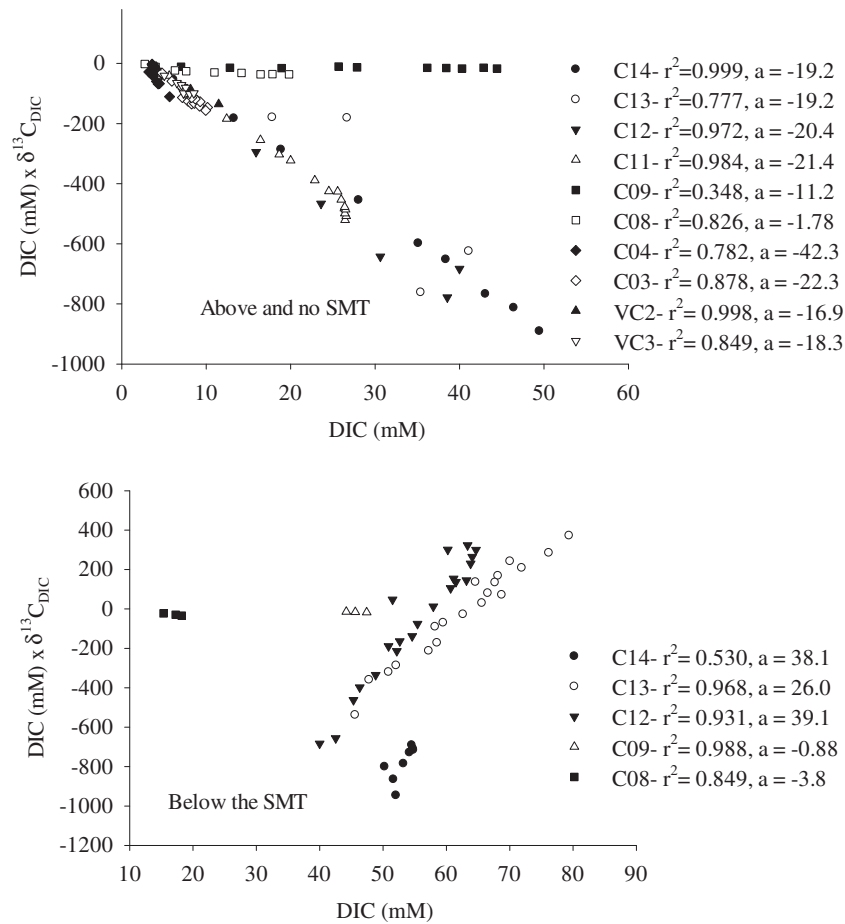


Figure 5. $\delta^{13}\text{C}_{\text{DIC}}$ as a function of the DIC concentration for evaluation of the DIC source at each core location. The upper panel reviews profiles above the SMT or if there was no SMT, through the entire core. The lower panel reviews cores below the SMT.

$\delta^{13}\text{C}_{\text{DIC}}$ at nearshore and offshore Hammerhead sites. Near-shore sites on the Hammerhead Line (VC02, VC03) had slight enrichment in DIC that may be from tundra C4 plants (Peterson et al., 1980). Offshore there was a strong $\delta^{13}\text{C}_{\text{DIC}}$ depletion (-42.3%) suggesting the source could be related to methane cycling and oxidation. Given low background methane concentrations and offshore location of this core, this pattern in DIC signature is likely from AOM over an extended period of time.

6. Conclusions

This study provides a thorough assessment of spatial variation in vertical CH_4 fluxes across the U.S. Alaskan Beaufort Shelf. Results reveal moderate vertical methane flux on the shelf relative to other regions in the Arctic Ocean, including those with high atmospheric CH_4 flux (Shakhova et al., 2005). Furthermore, the gas flux measure in this study was low relative to measurements above hydrate deposits in other coastal oceans (Table 3). There was a strong spatial variation in CH_4 diffusion though out the shallow sediments measured in this study. Eastward at the Hammerhead Line, very low diffusion rates were estimated from sediment porewater SO_4^{2-} profiles. Moving westward, a strong shift the SO_4^{2-} concentration slope coupled with a shallow sediment disappearance of CH_4 shows indicated elevated vertical methane flux. Highest vertical CH_4 fluxes were nearshore on the Cape Halkett Line and did decrease moving down slope. Spatial pattern in AOM levels along the Beaufort Shelf/Slope coincides with westward transport of

sediments during ice scouring. This would indicate that the CH_4 at this study location was formed since the last glaciation (Engels et al., 2008).

Methane release from shallow sediment has the potential to impact global climate (Dickens et al., 1995), however sources and relative contribution of ocean and tundra CH_4 is not well understood. In the Beaufort Sea-Mackenzie Delta, high methane hydrate loading is recognized as a potential atmospheric source (Osadetz and Chen, 2010). Recent studies do show significant CH_4 flux from sediment to atmosphere, up to 2500%–4400% super saturation in now submerged, former tundra regions around the East-Siberian and Laptev Sea (Shakhova et al., 2005). The source of this methane is not known and could easily be derived from non-hydrate organic carbon stores in degrading permafrost. Further, studies in Greenland and Antarctic ice cores from the Younger and Older Dryas periods with deuterium analysis of CH_4 suggest that methane hydrates are not significant contributors to methane increases during Quaternary, post-ice age, warming periods (Sower, 2006; Petrenko et al., 2009). Even if coastal sediment CH_4 that is mobilized during warming events (regardless of its source) is not significantly transported to the atmosphere, it may play a role in ocean carbon cycling and ocean ecology. Carbon isotope studies suggest CH_4 contribution to water column carbon cycling (Kelley et al., 1998; Cherrier et al., 1999). Determining the capacity for sediment and water column to assimilate CH_4 will support modeling to predict the implications of arctic methane releases.

Acknowledgments

Acknowledgment is made to the Office of Naval Research and Department of Energy, National Energy Technology Laboratory for support of this research. Acknowledgment is made to the Donors of the American Chemical Society Petroleum Research Fund for partial support of this research. We appreciate the persistent, strong support of the U.S. Coast Guard onboard science team during development of science plans and field work on the *USCGC Polar Sea*. Ray Boswell (NETL-DOE) provided an outstanding initial review of this manuscript. In addition, this manuscript was improved by the comments of two anonymous reviewers. This expedition was planned in collaboration with co-chief scientist Jens Greinert (GEOMAR Helmholtz Centre For Ocean Research Kiel) under the PERGAMON program.

References

- Aharon, P., Fu, B., 2000. Microbial sulfate reduction rates and sulfur and oxygen isotope fractionations at oil and gas seeps in deepwater Gulf of Mexico. *Geochim. Cosmochim. Acta* 64, 233–246.
- Aller, R.C., Blair, N.E., 2006. Carbon remineralization in the Amazon-Guianas tropical mobile mudbelt: a sedimentary incinerator. *Cont. Shelf Res.* 26, 2241–2259.
- Andreassen, K., Hart, P.E., MacKay, M., 1997. Amplitude versus offset modelling of the bottom simulating reflection associated with submarine gas hydrates. *Mar. Geol.* 137, 25–40.
- Arvidson, R.S., Morse, J.W., Joye, S.B., 2004. The sulfur biogeochemistry of chemosynthetic cold seep communities, Gulf of Mexico, USA. *Mar. Chem.* 87, 97–119.
- Belicka, L.L., Macdonald, R.W., Yunker, M.B., Harvey, H.R., 2004. The role of depositional regime on carbon transport and preservation in Arctic Ocean sediments. *Mar. Chem.* 86, 65–88.
- Berner, R.A., 1964. An idealized model of dissolved sulfate distribution in recent sediments. *Geochim. Cosmochim. Acta* 28, 1497–1503.
- Berner, R.A., 1978. Sulfate reduction and the rate of deposition of marine sediments. *Earth Planet. Sci. Lett.* 37, 492–498.
- Blair, N.E., Lethold, E.L., Ford, S.T., Peeler, K.A., Holmes, J.C., Perkey, D.W., 2003. The persistence of memory: the fate of ancient sedimentary organic carbon in a modern sedimentary system. *Geochim. Cosmochim. Acta* 67, 63–73.
- Biaostoch, A., Treude, T., Rüpke, L.H., Riebesell, U., Roth, C., Burwicz, E.B., Park, W., Latif, M., Böning, C.W., Madec, G., Wallmann, K., 2011. Rising Arctic Ocean temperatures cause gas hydrate destabilization and ocean acidification. *Geophys. Res. Lett.* 38, L08602. <http://dx.doi.org/10.1029/2011GL047222>.
- Boehme, S.E., Blair, N.E., Chanton, J.P., Martens, C.S., 1996. A mass balance of ^{13}C and ^{12}C in an organic-rich methane-producing marine sediment. *Geochim. Cosmochim. Acta* 60, 3835–3848.
- Boetius, A., Ravensschlag, K., Schubert, C.J., Rickert, D., Widdel, F., Gleske, A., Amann, R., Jørgensen, B.B., Witte, U., Pfannkuche, O., 2000. A marine microbial consortium apparently mediating anaerobic oxidation of methane. *Nature* 407, 623–626.
- Borowski, W.S., Paull, C.K., Ussler III, W., 1999. Global and local variations of interstitial sulfate gradients in the deep-water, continental margin sediments: sensitivity to underlying methane and gas hydrates. *Mar. Geol.* 159, 131–154.
- Borowski, W.S., Paull, C.K., Ussler III, W., 1996. Marine porewater sulfate profiles indicate in situ methane flux from underlying gas hydrate. *Geology* 24, 655–658.
- Boswell, R., Collett, T.S., 2011. Current perspectives on gas hydrate resources. *Energy Environ. Sci.* 4, 1206–1215.
- Brothers, L.L., Hart, P.E., Ruppel, C.D., 2012. Minimum distribution of subsea ice-bearing permafrost on the U.S. Beaufort Sea continental shelf. *Geophys. Res. Lett.* 39, L15501. <http://dx.doi.org/10.1029/2012GL052222>.
- Burdige, D.J., Komada, T., 2011. Anaerobic oxidation of methane and the stoichiometry of remineralization processes in continental margin sediments. *Limnol. Oceanogr.* 56, 1781–1796.
- Carmack, E.C., MacDonald, R.W., 2002. Oceanography of the Canadian shelf of the Beaufort Sea: a setting for marine life. *Arctic* 56, 29–45.
- Cherrier, J., Bauer, J.E., Druffel, E.R.M., Coffin, R.B., Chanton, J.P., 1999. Radiocarbon in marine bacteria: evidence for the ages of assimilated carbon. *Limnol. Oceanogr.* 44, 730–736.
- Coffin, R.B., Hamdan, L., Plummer, R., Smith, J., Gardner, J., Wood, W.T., 2008. Analysis of methane and sulfate flux in methane charged sediments from the Mississippi Canyon, Gulf of Mexico. *Mar. Petrol. Geol.* 25, 977–987.
- Coffin, R., Hamdan, L., Pohlman, J., Wood, W., Pecher, I., Henrys, S., Greinert, J., Faure, K., 2007. Geochemical Characterization of Concentrated Gas Hydrate Deposits on the Hikurangi Margin. Preliminary Geochemical Cruise Report, New Zealand. [NRL/MR/6110-08-9085](http://nrl.mr/6110-08-9085).
- Coffin, R.B., Pohlman, J.W., Gardner, J., Downer, R., Wood, W., Hamdan, L., Walker, S., Plummer, R., Gettrust, J., Diaz, J., 2006. Methane hydrate exploration on the mid Chilean coast: a geochemical and geophysical survey. *J. Pet. Sci. Eng.* 56, 32–41. <http://dx.doi.org/10.1016/j.petrol.2006.01.013>.
- Collett, T.S., 2009. Geologic and engineering controls on the production of permafrost-associated gas hydrate accumulations. In: Proceedings of the 6th International Conference on Gas Hydrates (ICGH 2008), Vancouver, British Columbia, CANADA, July 6–10, 2008.
- Dallimore, S.R., Collett, T.S., 1995. Intrapermafrost gas hydrates from a deep core hole in the Mackenzie Delta, Northwest Territories, Canada. *Geology* 23, 527–530.
- Dallimore, S.R., Collett, T.S., 1998. Gas hydrates associated with deep permafrost in the Mackenzie Delta, N.W.T., Canada: regional overview. In: *Permafrost-Seventh International Conference (Proceedings)*, Yellowknife (Canada). Collection Nordicana, vol. 55, pp. 201–206.
- Dickens, G.R., Koelling, M., Smith, D.C., Schieders, L., IODP Expedition 302 Scientists, 2007. Rhizon sampling of pore waters on scientific drilling expeditions: an example from the IODP Expeditions 302, Arctic Coring Expedition (ACEX). *Sci. Drill.* 4, 22–25.
- Dickens, G.R., 2001. Sulfate profiles and barium fronts in sediment on the Blake Ridge: present and past methane fluxes through a large gas hydrate reservoir. *Geochim. Cosmochim. Acta* 65, 529–543.
- Dickens, G.R., O'Neil, J.R., Rea, K.K., Owen, R.M., 1995. Dissociation of oceanic methane hydrate as a cause of the carbon isotope excursion at the end of Paleocene. *Paleoceanography* 10, 965–971.
- Dunton, K.H., Weingartner, T., Carmack, E.C., 2006. The near shore western Beaufort Sea ecosystem: circulation and importance of terrestrial carbon in arctic coastal food webs. *Prog. Oceanogr.* 71, 362–378.
- Engels, J.L., Edwards, M.H., Polyak, L., Johnson, P.D., 2008. Seafloor evidence for ice shelf flow across the Alaska-Beaufort margin of the Arctic Ocean. *Earth Surf. Process. Landforms* 33, 1047–1063.
- Frey, K., Smith, L.C., 2005. Amplified carbon release from vast West Siberian peatlands by 2100. *Geophys. Res. Lett.* 32, L09401.
- Gorham, E., 1991. Northern peatlands: role in the carbon cycle and probable responses to climatic warming. *Ecol. Appl.* 1, 182–195.
- Hamdan, L.J., Gillevet, P.M., Pohlman, J.W., Sikaroodi, M., Greinert, J., Coffin, R.B., 2011. Diversity and biogeochemical structuring of bacterial communities across the Porangahau ridge accretionary prism, New Zealand. *FEMS Microb. Ecol.* 77, 518–532.
- Hensen, C., Zabel, M., Pfeifer, K., Schwenk, T., Kasten, S., Riedinger, N., Schulz, H.D., Boetius, A., 2003. Control of sulfate porewater profiles by sedimentary events and the significance of anaerobic oxidation of methane for the burial of sulfur in marine sediments. *Geochim. Cosmochim. Acta* 67, 2631–2647.
- Hinrichs, K.-U., Hayes, J.M., Sylva, S.P., Brewer, R.G., DeLong, E.F., 1999. Methane-consuming archaeobacteria in marine sediments. *Nature* 398, 802–805.
- Hoehler, T.M., Borowski, W.S., Alperin, M.J., Rodriguez, N.M., Paull, C.K., 2000. Model stable isotope and radiocarbon characterization of anaerobic methane oxidation in gas hydrate-bearing sediments of the Blake Ridge. *Proc. Ocean Drill. Prog. Sci. Results* 164, 79–85.
- Isaksen, I.S.A., Gauss, M., Myhre, G., Anthony, K.M.W., Ruppel, C., 2011. Strong atmospheric chemistry feedback to climate warming from Arctic methane emissions. *Glob. Biogeochem. Cycl.* 25, 14. <http://dx.doi.org/10.1029/2010GB003845>. GB2002.
- Iversen, N., Jørgensen, B.B., 1993. Diffusion coefficients of sulfate and methane in marine sediments: influence of porosity. *Geochim. Cosmochim. Acta* 53, 571–578.
- Jørgensen, M.T., Brown, J., 2005. Classification of the Alaskan Beaufort Sea Coast and estimation of carbon and sediment inputs from coastal erosion. *Geo Mar. Lett.* 25, 69–80.
- Joye, S.B., Boetius, A., Orcutt, B.N., Montoya, R.P., Schulz, H.N., Ericson, M.J., Lugo, S.K., 2004. The anaerobic oxidation of methane and sulfate reduction in sediments from Gulf of Mexico cold seeps. *Chem. Geol.* 205, 219–238.
- Kelley, C.A., Coffin, R.B., Cifuentes, L.A., 1998. Stable isotope evidence for alternate carbon sources in the Gulf of Mexico. *Limnol. Oceanogr.* 43, 1962–1969.
- Knittel, K., Boetius, A., 2009. Anaerobic oxidation of methane: progress with an unknown process. *Ann. Rev. Microbiol.* 63, 311–334.
- Kvenvolden, K.A., 1999. Potential effects of gas hydrate on human welfare. *Proc. Nat. Acad. Sci. U. S. A.* 96, 3420–3426.
- Kvenvolden, K.A., 2002. Methane hydrate in the global organic carbon cycle. *Terra Nova* 14, 302–306.
- Lein, A.Y., Savvichev, A.S., Ivanov, M.V., 2011. Reservoir of dissolved methane in the water column of the sea of the Russian Arctic region. *Dokl. Earth Sci.* 441, 1576–1578.
- Lu, H., Matsumoto, R., 2005. Experimental studies on the possible influence of composition changes of pore water on the stability conditions of methane hydrate in marine sediments. *Mar. Chem.* 93, 149–157.
- Martens, C.S., Berner, R.A., 1974. Methane production in interstitial waters of sulfate-depleted marine sediments. *Science* 185, 1167–1169.
- Milkov, A.V., Sassen, R., 2003. Preliminary assessment of resources and economic potential of individual gas hydrate accumulations in the Gulf of Mexico continental slope. *Mar. Petrol. Geol.* 20, 111–128.
- Naidu, A.S., Mowatt, T.C., 1983. Sources and dispersal patterns of clay-minerals in surface sediments from the continental-shelf areas off Alaska. *Geol. Soc. Amer. Bull.* 94, 841–854.
- Orphan, V.J., House, C.H., Hinrichs, K.-U., McKeegan, K.D., DeLong, E.F., 2001. Methane-consuming archaea revealed by directly coupled isotopic and phylogenetic analysis. *Science* 293, 484–487.
- Oechel, W.C., Vourlitis, G.L., 1994. The effects of climate-change on land atmosphere feedbacks in Arctic tundra regions. *Trends Ecol. Evol.* 9, 324–329.
- Osadetz, K.G., Chen, Z., 2010. A re-evaluation of Beaufort Sea-Mackenzie Delta basin gas hydrate resource potential: petroleum system approaches to non-conventional gas resource appraisal and geologically-sourced methane flux. *Bull. Can. Petrol. Geol.* 58, 56–71.

- Pancost, R.D., Sinninghe Damsté, J.S., de Lint, S., van der Maarel, M.J.E.C., Cottschal, J.C., the Medinaut Shipboard Scientific Party, 2000. Biomarker evidence for widespread anaerobic methane oxidation in mediterranean sediments by a consortium of methanogenic Archaea and bacteria. *Appl. Environ. Microbiol.* 66, 1126–1132.
- Paull, C.K., Ussler III, W., Lorenson, T., Winters, W., Dougherty, J., 2005. Geochemical constraints on the distribution of gas hydrates in the Gulf of Mexico. *Geo Mar. Lett.* 25, 273–280.
- Petrenko, V.V., Smith, A.M., Brook, E.J., Lowe, D., Riedel, K., Brailsford, G., Hua, Q., Schaefer, H., Reeh, N., Weiss, R.F., Etheridge, D., Severinghaus, J.P., 2009. $^{14}\text{CH}_4$ measurements in Greenland ice: investigating last glacial termination CH_4 sources. *Science* 324, 506–508.
- Peterson, B.J., Howarth, R.W., Lipschultz, F., Ashendorf, D., 1980. Salt marsh detritus: an alternative interpretation of stable carbon isotope ratios and the fate of *Spartina alterniflora*. *Oikos* 34, 173–177.
- Plummer, R.E., Pohlman, J., Coffin, R.B., 2005. Compound-Specific Stable Carbon Isotope Analysis of Low-Concentration Complex Hydrocarbon Mixtures from Natural Gas Hydrate Systems. AGU, 86 52, Fall Meet. Suppl., 2005; Abstract OS43A-0608.
- Reimnitz, E., Barnes, P.W., 1974. Sea-ice as a geologic agent on the Beaufort Sea shelf of Alaska. In: Reed, J.C., Sater, J.E. (Eds.), *The Coast and Shelf of the Beaufort Sea*. Arctic Institute of North America, Arlington, VA, pp. 301–351.
- Ruppel, C., Dickens, G.R., Castellini, D.G., Gilhooly, W., Lizarralde, D., 2005. Heat and salt inhibition of gas hydrate formation in the northern Gulf of Mexico. *Geophys. Res. Lett.* 32, L04604. <http://dx.doi.org/10.1029/2004GL021909>.
- Seeberg-Elverfeldt, J., Koelling, M., Schluter, M., et al., 2005. Rhizon in Situ Sampler (RISS) for Pore Water Sampling from Aquatic Sediment, 230th National Meeting of the American-Chemical-Society, Washington, DC, AUG 28-SEP 01, 2005 Abstracts of papers of the American Chemical Society, p. 230. U1763-U1764 Meeting Abstract: 99-GEOC Published: AUG 28 2005.
- Shakhova, N., Semiletov, I., Panteleev, G., 2005. The distribution of methane on the Siberian Arctic shelves: implications for the marine methane cycle. *Geophys. Res. Lett.* 32, L09601. <http://dx.doi.org/10.1029/2005GL022751>.
- Shakhova, N.I., Semiletov, I., Leifer, I., Salyuk, A., Rekan, P., Kosmach, D., 2010. Geochemical and geophysical evidence of methane release over the East Siberian Arctic Shelf. *J. Geophys. Res.* 115, 14. <http://dx.doi.org/10.1029/2009JC005602>. C08007.
- Snyder, G.T., Hiruta, A., Matsumoto, R., Dickens, G.R., Tomaru, H., Takeuchi, R., Komatsubara, J., Ishida, Y., Yu, H., 2007. Pore water profiles and authigenic mineralization in shallow marine sediments above the methane-charged system on Umitaka Spur, Japan Sea. *Deep Sea Res. Part II: Top. Stud. Oceanogr.* 54, 1216–1239.
- Sower, T., 2006. Late quaternary atmospheric CH_4 isotope record suggests marine clathrates are stable. *Science* 311, 838–840.
- Torres, M.E., Bohrmann, G., Dube, T.E., Poole, F.G., 2003. Formation of modern and Paleozoic stratiform barite at cold methane seeps on continental margins. *Geology* 31, 897–900.
- Treude, T., Niggemann, J., Kallmeyer, J., Wintersteller, P., Schubert, C.J., Boetius, A., Jørgensen, B.B., 2005. Anaerobic oxidation of methane and sulfate reduction along the Chilean continental margin. *Geochem. Cosmochim. Acta* 69, 2767–2779.
- Valentine, D.L., Reeburgh, W.S., 2000. New perspectives on anaerobic methane oxidation. *Environ. Microbiol.* 2, 477–484.
- Valentine, D.L., 2002. Biogeochemistry and microbial ecology of methane oxidation in anoxic environments: a review. *Antonie Van Leeuwenhoek* 81, 271–282.
- Wehrmann, L.M., Risgaard-Petersen, N., Schrum, H.N., Walsh, E.A., Huh, Y., Ikehara, M., Pierre, C., D'Hondt, S., Ferdelman, R.G., Ravelo, A.C., Takahashi, K., Zarikian, C.A., The Integrated Ocean Drilling Program Expedition 323 Scientific Party, 2011. Couple organic and inorganic carbon cycling in the deep subseafloor sediment of the northeastern Bering Sea Slope (IODP Exp. 323). *Chem. Geol.* 284, 251–261.
- Whiticar, M.J., 1999. Carbon and hydrogen isotope systematics of bacterial formation and oxidation of methane. *Chem. Geol.* 16, 291–314.
- Zhang, C.L., Pancost, R.D., Sasseen, R., Qian, Y., Macko, S.A., 2003. Archeal lipid biomarkers and isotopic evidence of anaerobic methane oxidation associated with gas hydrates in the Gulf of Mexico. *Organ. Geochem.* 34, 827–836.